

# Contact Angle Measurements and Contact Angle Interpretation. 1. Contact Angle Measurements by Axisymmetric Drop Shape Analysis and a Goniometer Sessile Drop Technique

D. Y. Kwok,<sup>†,‡</sup> T. Gietzelt,<sup>§</sup> K. Grundke,<sup>§</sup> H.-J. Jacobasch,<sup>§</sup> and A. W. Neumann<sup>\*,†</sup>

Department of Mechanical Engineering, University of Toronto, 5 King's College Road, Toronto, Ontario, Canada M5S 3G8, and Institute of Polymer Research Dresden, Hohe Strasse 6, 01069 Dresden, Germany

Received August 13, 1996. In Final Form: March 12, 1997<sup>®</sup>

Low-rate dynamic contact angles and static advancing contact angles of 13 liquids were measured, respectively, by axisymmetric drop shape analysis (ADSA) and a conventional goniometer technique, on two copolymers, poly(propene-*alt*-*N*-(*n*-propyl)maleimide) and poly(propene-*alt*-*N*-(*n*-hexyl)maleimide); both have polar groups. In the case of the former technique for measuring contact angles (at very low velocity of the three-phase contact line), very complex contact angle responses were observed for some solid–liquid systems. In a specific case, slip and stick contact angle behavior occurs where the contact angle increases steadily by as much as 35° at constant three-phase contact radius and subsequently decreases sharply due to a sudden jump in the three-phase contact line. Thus, circumspection is necessary in the decision whether or not the experimental contact angles can be used to interpret surface energetics in conjunction with Young's equation and whether the solid–liquid systems violate the basic assumptions made in all surface energetics approaches. It was shown that if one omits the inconclusive contact angle measurements, the values of  $\gamma_{lv} \cos \theta$  change smoothly with  $\gamma_{lv}$  for these copolymers in a pattern already well-known for nonpolar surfaces. Goniometer and ADSA contact angle measurements were shown to be essentially identical for solid–liquid systems which have constant contact angles. In the specific case of the slip/stick mechanism using a goniometer for the contact angle measurements, the observed static advancing angle corresponds to the maximum angle of the entire slip/stick behavior, as registered by the automated axisymmetric drop shape analysis. Thus, conventional goniometer measurements may produce a mixture of meaningful and meaningless contact angles, with no criteria to distinguish between the two.

## Introduction

It is generally agreed that the measurement of contact angles on a given solid surface is the most practical way to obtain surface energetics (solid–vapor and solid–liquid surface tensions). At the centers of contact angle research is Young's equation

$$\gamma_{lv} \cos \theta_Y = \gamma_{sv} - \gamma_{sl} \quad (1)$$

which correlates the Young contact angle,  $\theta_Y$ , liquid–vapor surface tension,  $\gamma_{lv}$ , solid–vapor surface tension,  $\gamma_{sv}$ , and solid–liquid surface tension,  $\gamma_{sl}$ . Because only the liquid–vapor surface tension and the contact angle are directly measurable, according to the Young equation (1), one requires an additional equation (or other information) to determine  $\gamma_{sv}$  and  $\gamma_{sl}$ . Several approaches,<sup>1–8</sup> of current interest, were largely inspired by this idea in pursuit of

the determination of solid surface tensions from contact angles. Nevertheless, these approaches are, logically and conceptually, mutually exclusive.<sup>5</sup>

Experimentally, however, contact angle phenomena are also complicated and multifaceted.<sup>9–11</sup> The experimentally observed apparent contact angle,  $\theta$ , may or may not be equal to the Young contact angle,  $\theta_Y$ , in Young's equation<sup>10,11</sup>:

(1) On ideal solid surfaces, there is no contact angle hysteresis and the experimentally observed contact angle is equal to  $\theta_Y$ .

(2) On smooth but chemically heterogeneous solid surfaces,  $\theta$  is not necessarily equal to the thermodynamic equilibrium angle. Nevertheless, the experimental advancing contact angle,  $\theta_a$ , can be expected to be a good approximation of  $\theta_Y$ . Therefore, care must be exercised to ensure that the experimental apparent contact angle,  $\theta$ , is the advancing contact angle in order to be inserted into the Young equation.

(3) On rough solid surfaces, no such equality between advancing contact angle and  $\theta_Y$  exists. Thus, contact angles measured on rough surfaces cannot be used in conjunction with Young's equation.

In addition to these complexities, static and dynamic conditions, penetration of the liquid into the solid, swelling of the solid by the liquid, and chemical reactions can all

\* Author to whom correspondence should be addressed: fax, (416)-978-7753; e-mail, neumann@me.utoronto.ca.

<sup>†</sup> University of Toronto.

<sup>‡</sup> This paper represents, in part, the Ph.D. thesis of D. Y. Kwok.

<sup>§</sup> Institute of Polymer Research Dresden.

® Abstract published in *Advance ACS Abstracts*, May 1, 1997.

(1) Zisman, W. A. *Contact Angle, Wettability and Adhesion*; Advances in Chemistry Series; 43; American Chemical Society: Washington, DC, 1964.

(2) Fowkes, F. M. *Ind. Eng. Chem.* **1964**, *12*, 40.

(3) Driedger, O.; Neumann, A. W.; Sell, P. J. *Kolloid-Z. Z. Polym.* **1965**, *201*, 52.

(4) Neumann, A. W.; Good, R. J.; Hope, C. J.; Sejpal, M. *J. Colloid Interface Sci.* **1974**, *49*, 291.

(5) Spelt, J. K.; Li, D. The Equation of State Approach to Interfacial Tensions. In *Applied Surface Thermodynamics*; Neumann, A. W., Spelt, J. K., Eds.; Marcel Dekker, Inc.: New York, 1996; pp 239–292.

(6) Owens, D. K.; Wendt, R. C. *J. Appl. Polym. Sci.* **1969**, *13*, 1741.

(7) van Oss, C. J.; Chaudhury, M. K.; Good, R. J. *J. Chem. Rev.* **1988**, *88*, 927.

(8) Good, R. J.; van Oss, C. J. The Modern Theory of Contact Angles and the Hydrogen Bond Components of Surface Energies. In *Modern Approaches to Wettability: Theory and Applications*; Schrader, M., Loeb, G., Eds.; Plenum Press: New York, 1992; pp 1–27.

(9) Neumann, A. W. *Adv. Colloid Interface Sci.* **1974**, *4*, 105.

(10) Marmur, A. *Colloids Surf. A* **1996**, *116*, 25.

(11) Li, D.; Neumann, A. W. Thermodynamic Status of Contact Angles. In *Applied Surface Thermodynamics*; Neumann, A. W., Spelt, J. K., Eds.; Marcel Dekker, Inc.: New York, 1996; pp 109–168.

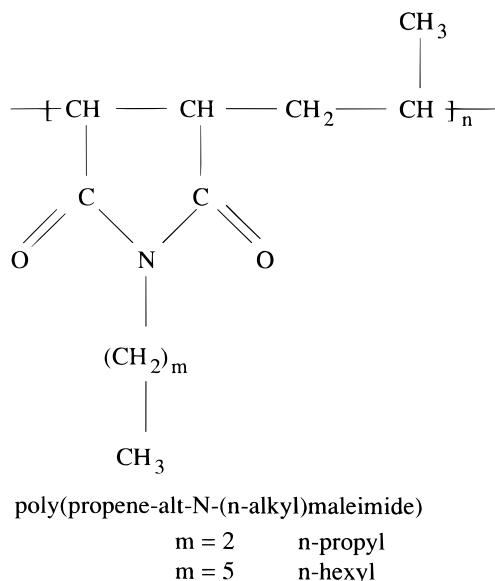


**Figure 1.** Chemical structure of the copolymers with polar groups: poly(propene-*alt*-*N*-(*n*-alkyl)maleimide).

play a role. For example, swelling of the solid by the liquid<sup>12</sup> can change the solid in an unknown manner and affect the values of  $\gamma_{sl}$  and possibly  $\gamma_{sv}$  and, hence, the apparent contact angle,  $\theta$ . While such effects do not necessarily imply that Young's equation is not applicable, they change the solid/liquid interfacial tension(s) as a function of time and would then violate assumptions made in all surface energetics approaches,<sup>1-8</sup> such as constancy of  $\gamma_{sv}$  when going from liquid to liquid, or  $\gamma_{sl} = \text{constant}$ , i.e., invariant with time. For that reason, measurements which show a systematic change in contact angle, even when  $\gamma_{lv} = \text{constant}$ , have to be discarded.

The existence of these various effects is well-known, but they have not been looked at and investigated systematically. Typically, contact angles are measured simply by depositing a drop of liquid on a given solid surface, and placing a tangent to the drop at its base using, for example, a goniometer. Such a primitive procedure cannot be expected to reflect the complexities of solid-liquid interactions. It is, therefore, the purpose of this paper to illustrate experimentally the complexity of contact angle phenomena on two copolymer surfaces with polar groups, which present more scope for such interactions than inert surfaces, and to demonstrate experimentally how contact angle data obtained by conventional strategies may be misleading in the interpretation of solid surface tensions using the approaches<sup>1-8</sup> of current interest. A body of contact angle data are reported using two different contact angle techniques: axisymmetric drop shape analysis—profile (ADSA-P) and, to prove our point, a goniometer technique.

### Materials (Solid Surface and Liquids)

Two copolymers, poly(propene-*alt*-*N*-(*n*-propyl)maleimide) and poly(propene-*alt*-*N*-(*n*-hexyl)maleimide), i.e., copolymers with different side chains, were used for contact angle measurements (see Figure 1 for chemical structure). The polymers were prepared by polymer analogous reactions for alternating poly(propene-maleic anhydride) copolymer with propyl- or hexylamine.<sup>13</sup> The molecular weights of the poly(propene-maleic anhydride) copolymer determined by gel permeation chromatography

are  $M_w = 27\,300$  g/mol and  $M_n = 9700$  g/mol, respectively. For calibration a poly(propene-maleic anhydride) copolymer was used with known molecular weight ( $M_w = 62\,500$  g/mol,  $M_n = 16\,100$  g/mol). It should be noted that excess of primary amines was used in the preparation of the copolymers; the maleimides are expected to convert 100% to the propyl- and hexylmaleimides. Subsequently, the copolymers were dissolved in tetrahydrofuran and precipitated using hexane. The procedure was repeated several times.

For each copolymer, a 2% solution was prepared using tetrahydrofuran (Sigma-Aldrich, 99.9+% HPLC) as the solvent. Silicon wafers (100) (Silicon Sense, Nashua, NH) were selected as the substrate for the contact angle measurements. They were obtained as circular disks of about 10 cm diameter and were cut into rectangular shapes of about 2.5 cm  $\times$  5 cm. Each rectangular silicon wafer surface was then soaked in chromic acid for at least 24 h, rinsed with doubly-distilled water, and dried under a heat lamp before the polymer coating. A few drops of the 2% copolymer/tetrahydrofuran solution were deposited on the dried silicon wafers inside glass dishes overnight; the solution spread and a thin layer of the copolymer formed on the wafer surface after tetrahydrofuran evaporated. This preparation produced good quality coated surfaces, as manifested by light fringes, due to refraction at these surfaces, suggesting that roughness is in the order of nanometers or less.

In the case of axisymmetric drop shape analysis—profile (ADSA-P) as the contact angle technique, a hole of about 2 mm diameter was made, by using a diamond drill bit (SMS-0.027) from Lunzer, NY, in the center of each rectangular wafer surface before soaking in chromic acid. Such an arrangement allows formation of the sessile drop by supplying liquid from below the surface using a motorized syringe mechanism.<sup>14</sup> Oliver et al.<sup>15,16</sup> pioneered this strategy to measure sessile drop contact angles because of its potential for avoiding drop vibrations, which might lead inadvertently to receding contact angles.

Thirteen liquids were chosen in this study. Selection of these liquids was based on the following criteria: (1) liquids should include a wide range of intermolecular forces; (2) liquids should be nontoxic; and (3) the liquid surface tension should be higher than the anticipated solid surface tension.<sup>1,5,17</sup> They are, in the order of increasing surface tension, *cis*-decalin, 2,5-dichlorotoluene, ethyl cinnamate, dibenzylamine, dimethyl sulfoxide (DMSO), 1-bromonaphthalene, diethylene glycol, ethylene glycol, diiodomethane, thiodiethanol, formamide, glycerol, and water. The physical properties and surface tensions of these liquids are shown in Table 1, for room temperature,  $24 \pm 1$  °C. The four significant figures reported in Table 1 are meant to illustrate the consistency and precision of our surface tension measurements, not the accuracy of the liquid surface tensions.

### Methods and Procedures

**Axisymmetric Drop Shape Analysis—Profile (ADSA-P).** ADSA-P is a technique to determine liquid-fluid interfacial tensions and contact angles from the shape of axisymmetric menisci, i.e., from sessile as well as pendant drops. Assuming that the experimental drop is Laplacian and axisymmetric, ADSA-P finds the theoretical profile that best matches the drop profile extracted from the image

(14) Kwok, D. Y.; Lin, R.; Mui, M.; Neumann, A. W. *Colloids Surf. A* **1996**, *116*, 63.

(15) Oliver, J. F.; Huh, C.; Mason, S. G. *J. Colloid Interface Sci.* **1977**, *59*, 568.

(16) Oliver, J. F.; Huh, C.; Mason, S. G. *Colloids Surf.* **1980**, *1*, 79.

(17) Grundke, K.; Bogumil, T.; Gietzelt, T.; Jacobasch, H.-J.; Kwok, D. Y.; Neumann, A. W. *Prog. Colloid Polym. Sci.* **1996**, *101*, 58.

(12) Sedev, R. V.; Petrov, J. G.; Neumann, A. W. *J. Colloid Interface Sci.* **1996**, *180*, 36.

(13) Wienhold, U. Ph.D. Thesis, Martin-Luther-Universität Halle-Wittenberg, Germany, 1994.

**Table 1. Density, Purity, and Surface Tension of the Liquids Used at Room Temperature**

liquids	supplier	purity	density (g/cm <sup>3</sup> )	surface tension $\gamma_{lv}$ (mJ/m <sup>2</sup> )	no. of drops
cis-decalin	Aldrich	99%	0.897	32.32 $\pm$ 0.01	7
2,5-dichlorotoluene	Aldrich	98%	1.254	34.64 $\pm$ 0.003	10
ethyl cinnamate	Aldrich	99%	1.049	37.17 $\pm$ 0.02	10
dibenzylamine	Aldrich	97%	1.026	40.80 $\pm$ 0.06	9
DMSO	Sigma-Aldrich	99.9% (HPLC)	1.101	42.68 $\pm$ 0.09	10
1-bromonaphthalene	Aldrich	98%	1.489	44.31 $\pm$ 0.05	7
diethylene glycol	Aldrich	99%	1.118	44.68 $\pm$ 0.03	9
ethylene glycol	Aldrich	99+%	1.113	47.55 $\pm$ 0.02	10
diiodomethane	Aldrich	99%	3.325	49.98 $\pm$ 0.02	10
thiodiethanol	Aldrich	99+%	1.221	56.26 $\pm$ 0.004	10
formamide	Aldrich	99.5+%	1.134	59.08 $\pm$ 0.01	10
glycerol	Baker Analyzed	99.8%	1.258	65.02 $\pm$ 0.04	8
water	LAST <sup>a</sup>	doubly distilled	0.997	72.70 $\pm$ 0.09	10

<sup>a</sup> Laboratory of Applied Surface Thermodynamics.

of a real drop, from which the surface tension, contact angle, drop volume, and surface area can be computed. The strategy employed is to fit the shape of an experimental drop to a theoretical drop profile according to the Laplace equation of capillarity, using surface/interfacial tension as adjustable parameter. The best fit identifies the correct surface/interfacial tension from which the contact angle can be determined by a numerical integration of the Laplace equation. Details of the methodology and experimental setup can be found elsewhere.<sup>14,18–20</sup>

Sessile drop experiments were performed by ADSA-P to determine contact angles at room temperature. However, it has been found that since ADSA assumes an axisymmetric drop shape, the values of liquid surface tensions measured from sessile drops are very sensitive to even a very small amount of surface imperfection, such as roughness and heterogeneity, while contact angles are less sensitive. Therefore, the liquid surface tensions used in this study were measured by applying ADSA-P to a pendant drop. Results of the liquid surface tension are shown in Table 1.

Sessile drop contact angle measurements using ADSA-P were performed dynamically, by using a motor-driven syringe to pump liquid steadily into the sessile drop from below the surface.<sup>14</sup> In this study, at least 5 and up to 10 dynamics contact angle measurements were performed for each liquid, at velocities of the three-phase contact line less than 0.6 mm/min. The choice of this velocity range was based on previous studies:<sup>14,21,22</sup> it has been shown that low-rate dynamic contact angles at this velocity range are essentially identical to the static contact angles, at least for these relatively smooth surfaces.

In actual experiments, an initial liquid drop of about 0.3 cm radius was carefully deposited, covering the hole on the surface. This is to ensure that the drop will increase axisymmetrically in the center of the image field when liquid is supplied from the bottom of the surface and will not hinge on the lip of the hole. The motor in the motorized syringe mechanism was then set to a specific speed, by adjusting the voltage from a voltage controller. Such a syringe mechanism pushes the syringe plunger, leading to an increase in drop volume and hence the three-phase contact radius. A sequence of pictures of the growing drop

was then recorded by the computer typically at a rate of one picture every 2 s, until the three-phase contact radius was about 0.5 cm or larger. For each low-rate dynamic contact angle experiment, at least 50 and up to 100 pictures were normally taken. Since ADSA-P determines the contact angle and the three-phase contact radius simultaneously for each picture, the advancing dynamic contact angles as a function of the three-phase contact radius (i.e. location on the surface) can be obtained. The actual rate of advancing can be determined by linear regression, by plotting the three-phase contact radius over time. Different rates of advancing were studied, by adjusting the speed of the pumping mechanism.

It should be noted that measuring contact angles as a function of the three-phase contact radius has an additional advantage: the quality of the surface is observed indirectly in the measured contact angles. If a solid surface is not very smooth, irregular and inconsistent contact angle values will be seen as a function of the three-phase contact radius. When the measured contact angles are essentially constant as a function of surface location, the mean contact angle for a specific rate of advancing can be obtained by averaging the contact angles, after the three-phase contact radius reaches 0.4–0.5 cm (see later). The purpose of choosing these relatively large drops is to avoid any line tension effects on the measured contact angles.<sup>23–25</sup>

**Goniometer Technique.** A conventional goniometer equipped with an eye-piece was also used. A syringe connected to a Teflon capillary of about 2 mm inner diameter was used to supply liquid into the sessile drop from above. A sessile drop of about 0.4–0.5 cm radius was used. The three-phase contact line of the drop was then slowly advanced by supplying more liquid from above through the capillary which was always kept in contact with the drop. The maximum (advancing) contact angles were measured carefully from the left and right side of the drop and subsequently averaged. The above procedures were repeated for five drops on five new surfaces. All readings were then averaged to give an averaged contact angle. All experiments were performed at room temperature.

## Results and Discussion

**ADSA-P Measurements.** *Poly(propene-alt-N-(n-propyl)maleimide)*. Figure 2a shows a typical example of a low-rate dynamic contact angle experiment of water on a poly(propene-alt-N-(n-propyl)maleimide) copolymer surface. As can be seen in this figure, increasing the drop

(18) Rotenberg, Y.; Boruvka, L.; Neumann, A. W. *J. Colloid Interface Sci.* **1983**, *93*, 169.

(19) Cheng, P.; Li, D.; Boruvka, L.; Rotenberg, Y.; Neumann, A. W. *Colloids Surf.* **1983**, *93*, 169.

(20) Lahooti, S.; del Rio, O. I.; Cheng, P.; Neumann, A. W. Axisymmetric Drop Shape Analysis. In *Applied Surface Thermodynamics*; Neumann, A. W., Spelt, J. K., Eds.; Marcel Dekker, Inc.: New York, 1996; pp 441–507.

(21) Kwok, D. Y.; Budziak, C. J.; Neumann, A. W. *J. Colloid Interface Sci.* **1995**, *173*, 143.

(22) Kwok, D. Y.; Li, D.; Neumann, A. W. Capillary Rise at a Vertical Plate as a Contact Angle Technique. In *Applied Surface Thermodynamics*; Neumann, A. W., Spelt, J. K., Eds.; Marcel Dekker, Inc.: New York, 1996; pp 413–440.

(23) Li, D.; Neumann, A. W. *Adv. Colloid Interface Sci.* **1992**, *39*, 347.

(24) Duncan, D.; Li, D.; Gaydos, J.; Neumann, A. W. *J. Colloid Interface Sci.* **1995**, *169*, 256.

(25) Gaydos, J.; Neumann, A. W. Line Tension in Multiphase Equilibrium Systems. In *Applied Surface Thermodynamics*; Neumann, A. W., Spelt, J. K., Eds.; Marcel Dekker, Inc.: New York, 1996; pp 169–238.

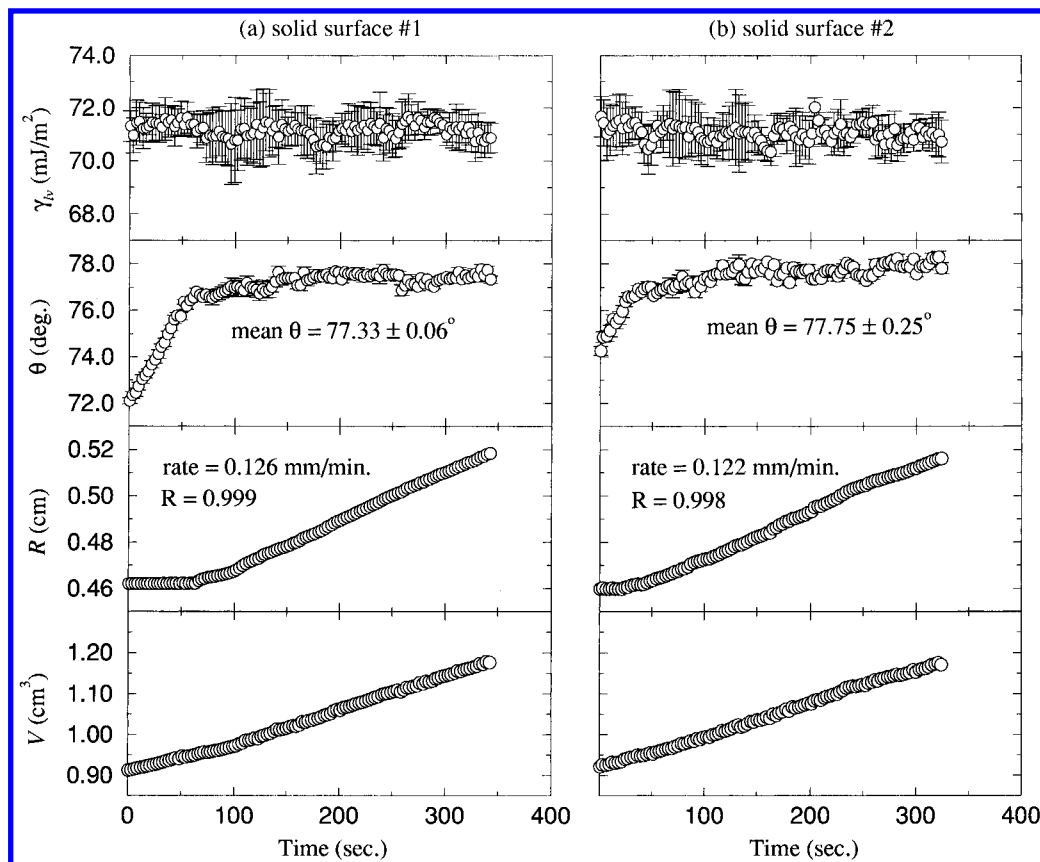


**Figure 2.** Low-rate dynamic contact angles of water on poly(propene-*alt*-*N*-(*n*-propyl)maleimide) copolymer measured by ADSA-P.  $\gamma_{lv}$ ,  $\theta$ ,  $R$ , and  $V$  are, respectively, the liquid-vapor surface tension, contact angle, three-phase contact radius, and drop volume.

volume,  $V$ , linearly from 0.9 to about 1.2 cm<sup>3</sup> increases the apparent contact angle,  $\theta$ , from about 72° to 77° at essentially constant three-phase contact radius,  $R$ . This is due to the fact that even carefully putting an initial water drop from above on a solid surface can result in a contact angle somewhere between advancing and receding. This effect is more pronounced for liquids, such as water, which evaporate fast. Thus, it takes time for the initial drop front to start advancing. Further increase in the drop volume causes the three-phase contact line to advance, with  $\theta$  essentially constant as  $R$  increases. Increasing the drop volume in this manner ensures the measured  $\theta$  to be an advancing contact angle. It should be noted that the liquid-vapor surface tensions calculated by ADSA-P sessile drop are fairly constant, but not as reliable as pendant drop, as explained above. The rate of advancing for this experiment and other liquids can be determined by linear regression from the linear region of the plot of the three-phase contact radius,  $R$ , over time: it was found that the drop periphery was being advanced at a rate of 0.13 mm/min, in the specific example given in Figure 2a. The regression coefficient for the rate of advancing was found to be 0.999; this indicates that the rate of change of the three-phase contact line was very constant, even though it was controlled only by manipulating the drop volume.

It should be noted that, in this specific example, the measured contact angles are essentially constant as  $R$  increases. This indicates good surface quality of the surfaces used. It turns out that averaging the measured contact angles after  $R$  reaches 0.48 cm is convenient, since the drop is guaranteed to be in the advancing mode and that line tension effects are negligible.<sup>23–25</sup> Averaging the measured contact angles, after  $R$  reaches 0.48 cm, yields a mean contact angle of  $77.33 \pm 0.06^\circ$ . The error limit in this case and the rest of the paper is the 95% confidence interval. While a three-phase contact radius

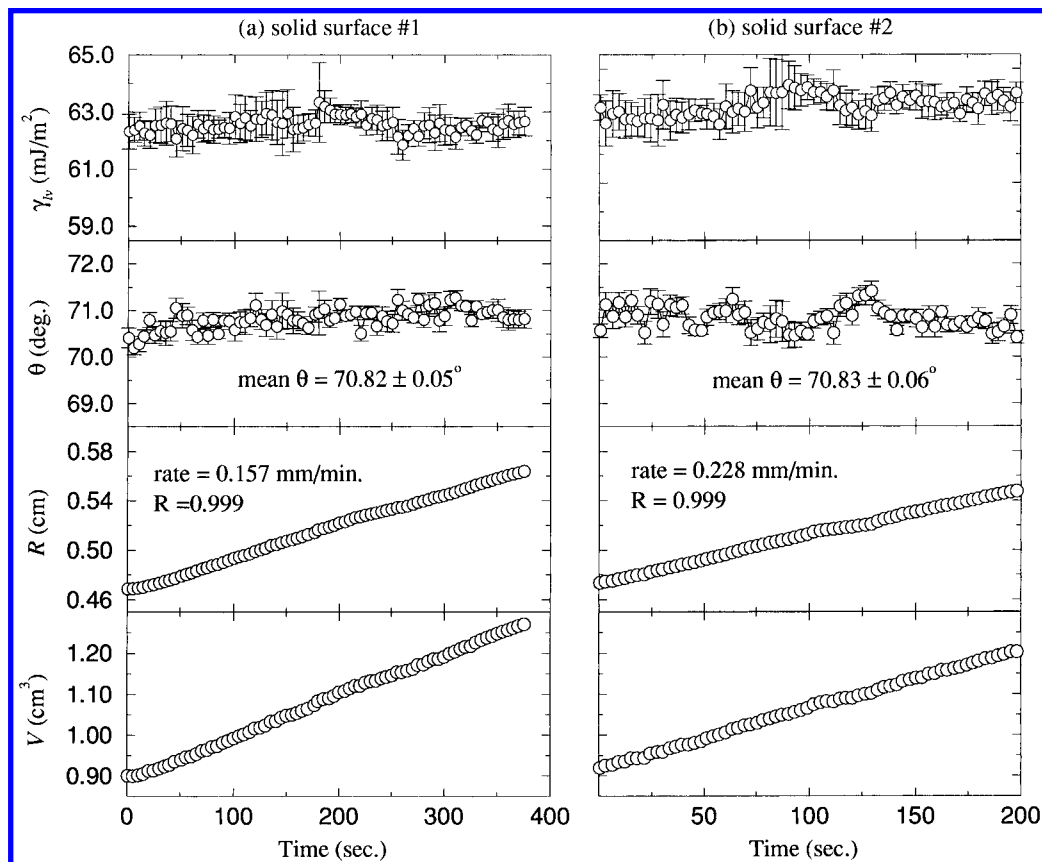
of 0.48 cm may seem to be an arbitrary value, it turns out that there is virtually no dependence on the choice of the starting point. The reproducibility of this solid-liquid system is shown in Figure 2b, for a different solid surface, at a slightly different rate of advancing of 0.12 mm/min. The mean  $\theta$  in this experiment is found to be  $77.75 \pm 0.25^\circ$ . While the contact angles thus obtained in the two experiments agree very well, it is also apparent that the contact angles immediately after drop deposition differ by as much as 2°. A total of nine experiments at different rates of advancing were performed for water, each on a newly prepared surface. The results of these low-rate dynamic contact angles are summarized in Table 2, together with similar results for other liquids. Since the contact angles of water at different rates of advancing (in Table 2) are essentially constant, they can be averaged and result in a final value for  $\theta$  of  $77.51 \pm 0.27^\circ$ . It should be noted that the 95% confidence calculated in this manner includes all possible variations, e.g., due to errors of the experiments, experimental technique, and solid surface preparation.

Figure 3 shows two contact angle experiments of glycerol at different rates of advancing. Because the contact angles are essentially constant for all experiments, they can be averaged, resulting in mean contact angles of  $70.82 \pm 0.05^\circ$  and  $70.83 \pm 0.06^\circ$ , respectively, at rates of advancing of 0.16 and 0.23 mm/min. A total of eight experiments (for eight different rates of advancing) were performed on a new solid surface each time. The results are also summarized in Table 2.

In Figure 4, two contact angle experiments of formamide are shown at different rates of motion of the three-phase contact line. It can be seen in Figure 4a that as the drop volume increases initially, the contact angle increases from 60° to 63° at essentially constant three-phase contact radius. As the drop volume continues to increase,  $\theta$  suddenly decreases to 60° and the three-phase contact

**Table 2. Low-Rate Dynamic Contact Angles of Different Liquids on Poly(propene-*alt*-*N*-(*n*-propyl)maleimide) Copolymer Surface**

water		glycerol		thiodiethanol		1-bromonaphthalene	
rate (mm/min)	$\theta$ (deg)	rate (mm/min)	$\theta$ (deg)	rate (mm/min)	$\theta$ (deg)	rate (mm/min)	$\theta$ (deg)
0.054	77.46	0.083	70.79	0.090	53.92	0.484	30.85
0.064	78.08	0.115	70.94	0.127	54.22	0.490	30.66
0.067	77.07	0.121	70.77	0.128	54.21	0.499	30.55
0.068	77.79	0.157	70.82	0.157	53.82	0.599	30.62
0.110	77.58	0.182	70.58	0.234	54.12	0.532	30.93
0.114	76.98	0.192	70.35	0.250	53.94	0.557	30.87
0.122	77.75	0.201	70.28			0.570	30.67
0.126	77.33	0.228	70.83			0.602	30.70
0.148	77.58					0.633	30.90
$77.51 \pm 0.27^a$		$70.67 \pm 0.20^a$		$54.04 \pm 0.18^a$		$30.75 \pm 0.11^a$	

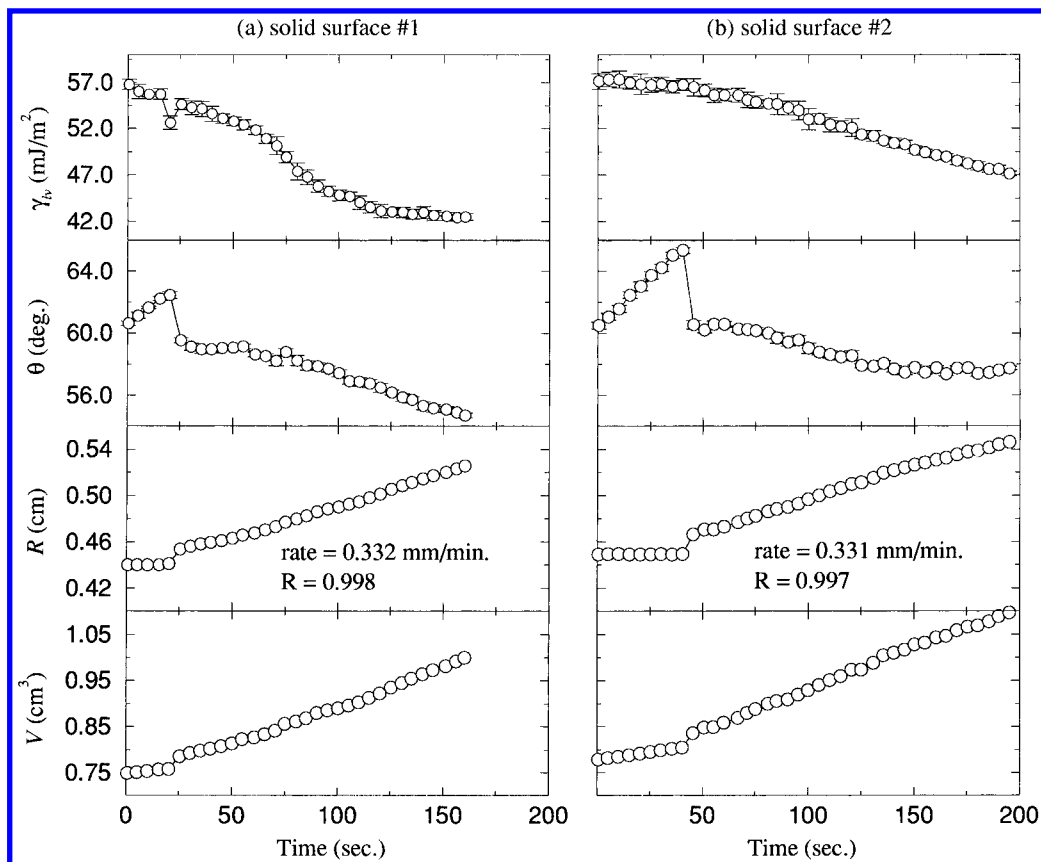
<sup>a</sup> Mean value.**Figure 3.** Low-rate dynamic contact angles of glycerol on poly(propene-*alt*-*N*-(*n*-propyl)maleimide) copolymer measured by ADSA-P.

line starts to move. When  $R$  increases further, the contact angle decreases slowly from  $60^\circ$  to  $54^\circ$ . Focusing on the surface tension–time plot indicates that the surface tension of formamide decreases with time. One possible explanation is that dissolution of the copolymer occurs, causing the liquid–vapor surface tension to change from that of the pure liquid. Similar behavior for a different experiment (at nearly the same rate of advancing) is shown in Figure 4b. It is an important question to ask which contact angles one should use for the interpretation in terms of surface energetics. Since chemical or physical reactions such as polymer dissolution change the liquid–vapor, solid–vapor, and solid–liquid interface (interfacial tensions) in an unknown manner, such a question is very difficult to answer. Because we are unsure whether or not the solid–vapor surface tension,  $\gamma_{sv}$ , will remain constant and whether Young's equation is applicable, these contact angle data should be disregarded for the interpretation in terms of surface energetics, since all approaches<sup>1–8</sup> assume the constancy of  $\gamma_{sv}$  going from

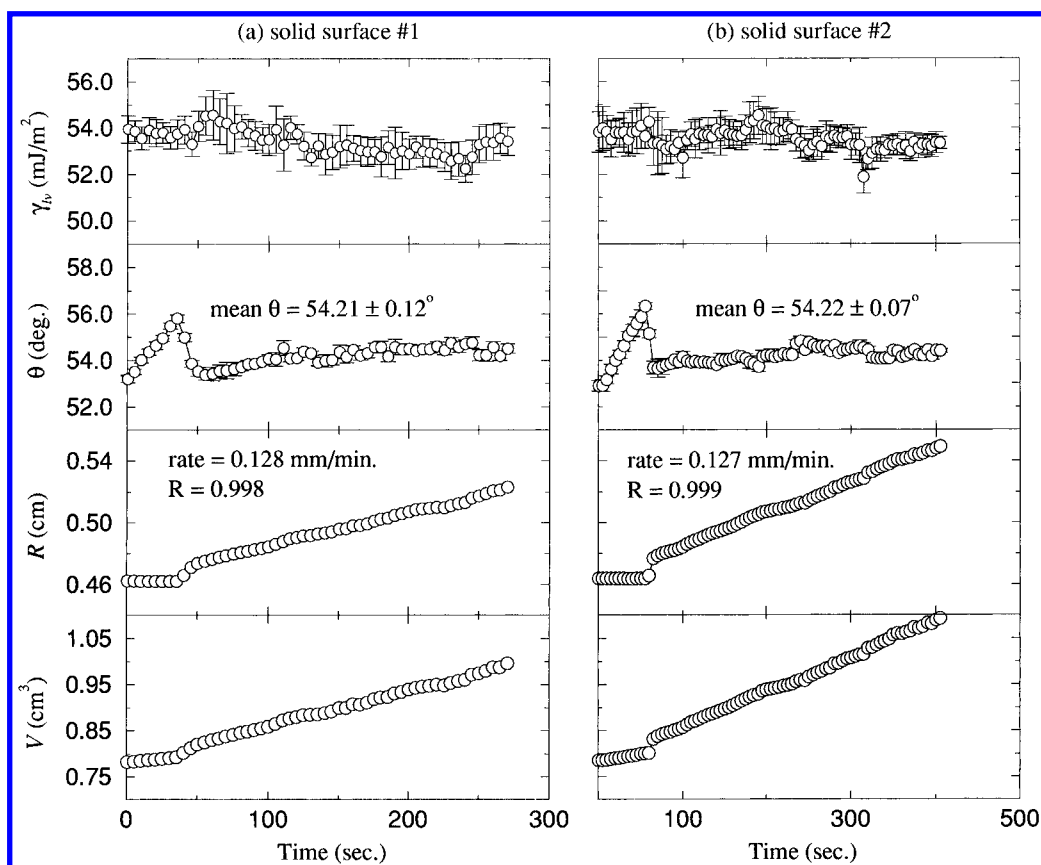
liquid to liquid and the validity of Young's equation, as discussed before.

Figure 5 shows two contact angle experiments of thiodiethanol. A slightly different contact angle response is observed: slip/stick behavior occurs at the beginning of the experiment but not once the three-phase contact line has started to move. The mean contact angle can be obtained from the region where  $\theta$  is nearly constant. This results in a mean  $\theta$  of  $54.21 \pm 0.12^\circ$  at a rate of 0.13 mm/min in Figure 5a. To illustrate the reproducibility of this experiment, a second experiment performed at nearly the same rate is shown in Figure 5b, where similar contact angle behavior is also observed. The mean contact angle in this specific case is found to be  $54.22 \pm 0.07^\circ$ , which is essentially identical to that obtained in Figure 5a. A summary of all contact angle results for thiodiethanol is shown in Table 2, at six different rates of change of the three-phase contact radius.

Contact angle results of diiodomethane for two different experiments are shown in Figure 6. It can be seen in



**Figure 4.** Low-rate dynamic contact angles of formamide on poly(propene-*alt*-*N*-(*n*-propyl)maleimide) copolymer surface measured by ADSA-P. The decrease in the  $\gamma_{sv}$  suggests the dissolution of the copolymer by the liquid.



**Figure 5.** Low-rate dynamic contact angles of thiodiethanol on poly(propene-*alt*-*N*-(*n*-propyl)maleimide) copolymer measured by ADSA-P.

Figure 6a that initially the apparent drop volume, as perceived by ADSA-P, increases linearly, and the contact angle increases from  $45^\circ$  to  $65^\circ$  at essentially constant

three-phase contact radius. Suddenly, the drop front jumps to a new location as more liquid is supplied into the sessile drop. The resulting contact angle decreases sharply



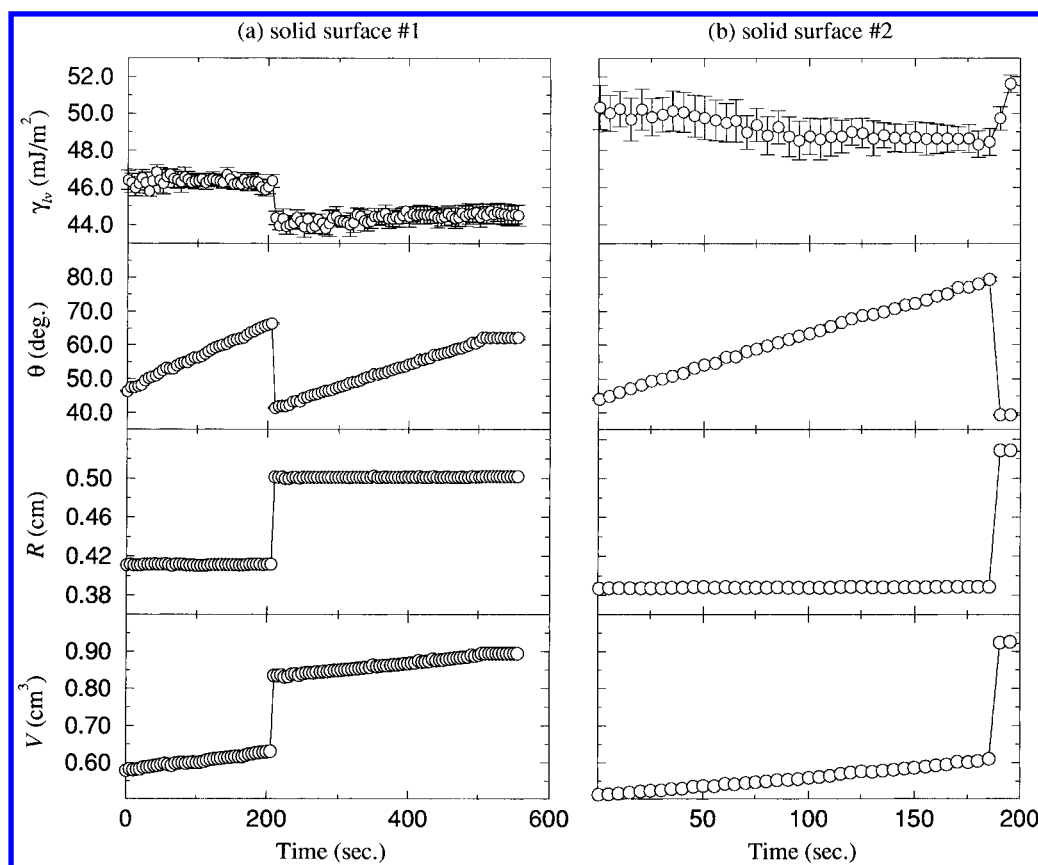


**Figure 6.** Low-rate dynamic contact angles of diiodomethane on poly(propene-*alt*-*N*-(*n*-propyl)maleimide) copolymer measured by ADSA-P. It should be noted that not all contact angles from this slip/stick behavior can be used in conjunction with Young's equation (see text).

from 65° to 40°. As more liquid is supplied into the sessile drop, the contact angle increases again. Such slip/stick behavior could be due to noninertness of the surface. Phenomenologically, an energy barrier for the drop front exists, resulting in sticking, which causes  $\theta$  to increase at constant  $R$ . However, as more liquid is supplied into the sessile drop, the drop front possesses enough energy to overcome the energy barrier, resulting in slipping, which causes  $\theta$  to decrease suddenly. It should be noted that as the drop front jumps from one location to the next, it is unlikely that the drop will remain axisymmetric. Such a nonaxisymmetric drop will obviously not meet the basic assumptions underlying ADSA-P, causing possible errors, e.g., in the apparent surface tension and drop volume. This can be seen from the discontinuity of the apparent drop volume and apparent surface tension with time as the drop front sticks and slips. A similar experiment for a new surface, with similar results, is shown in Figure 6b. Obviously, the observed contact angles in Figure 6 cannot all be Young contact angles, since  $\gamma_{sv}$  and  $\gamma_{lv}$  (and  $\gamma_{sl}$ ) are constants, so that because of Young's equation,  $\theta$  ought to be a constant. In addition, it is difficult to decide unambiguously at this moment whether or not Young's equation is applicable at all because of lack of understanding of the slip/stick mechanism. Therefore, these contact angles should not be used for the interpretation in terms of surface energetics.

The results of ethylene glycol for two different experiments are shown in Figure 7. It can be seen in Figure 7a that the contact angle increases slowly from 54° to 57° as the three-phase contact line advances from 0.46 to 0.54 cm. While the cause of this increase in the contact angle is unclear, it is suspected that the solid-liquid interfacial tension is changed slowly due to physicochemical reaction: according to Young's equation, if the values of  $\gamma_{lv}$  and  $\gamma_{sv}$  are constant, a change in the contact angle must

be a consequence of a change in  $\gamma_{sl}$ . A similar experiment, with similar results, is shown in Figure 7b. It should be noted that the observed trends in the contact angle may well start immediately after drop formation, not only after the measurement procedure was set in motion. Also, there is no reason to suspect that the change of contact angle with time (or radius) would cease once the measurement was terminated. More likely, such trends would continue. Because there is no unique apparent contact angle and it is unclear whether or not the solid-vapor surface tension will remain constant and whether Young's equation is applicable, these angles should be excluded from the interpretation in terms of surface energetics. However, one might consider averaging the contact angles larger than  $R = 0.48$  cm, since  $\gamma_{lv}$  seems to be constant and since the contact angle error after averaging would not be very large, i.e.,  $\theta = 55.74 \pm 0.63^\circ$ . It should be noted that such averaging is not allowed: apart from the experimental reasons given above, the question of whether averaging over some data is allowed or not has firm quantitative answers based on the laws of statistics. The statistical justification for disregarding this and other similar systems is discussed in the Appendix. The main fact is that the statistical analysis rejects "averaging" of the above contact angle data over time by a very large margin.

Figure 8 shows the contact angle results of diethylene glycol for two different experiments. As can be seen in both parts a and b of Figure 8, the contact angle responses of diethylene glycol are very similar to those in Figure 7 for ethylene glycol on this copolymer. In Figure 8a, the contact angle slowly increases from about 45° to 49° as the three-phase contact line advances. Another experiment, with similar results, is shown in Figure 8b. Since diethylene glycol and ethylene glycol are chemically similar, it is not surprising to see contact angle responses essentially identical to those in Figure 7. Again, the

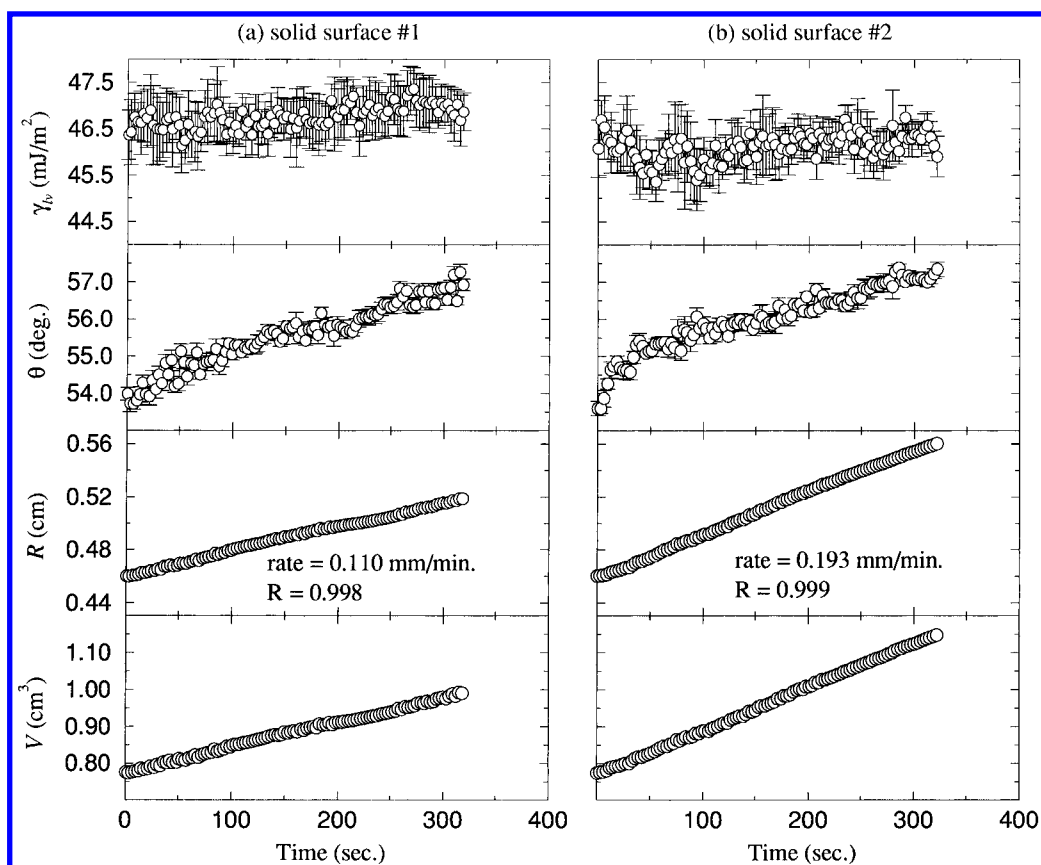


**Figure 7.** Low-rate dynamic contact angles of ethylene glycol on poly(propene-*alt*-*N*-(*n*-propyl)maleimide) copolymer measured by ADSA-P. It is suspected that the solid-liquid (and/or solid-vapor) interfacial tensions are changed slowly due to physicochemical reaction (see text).

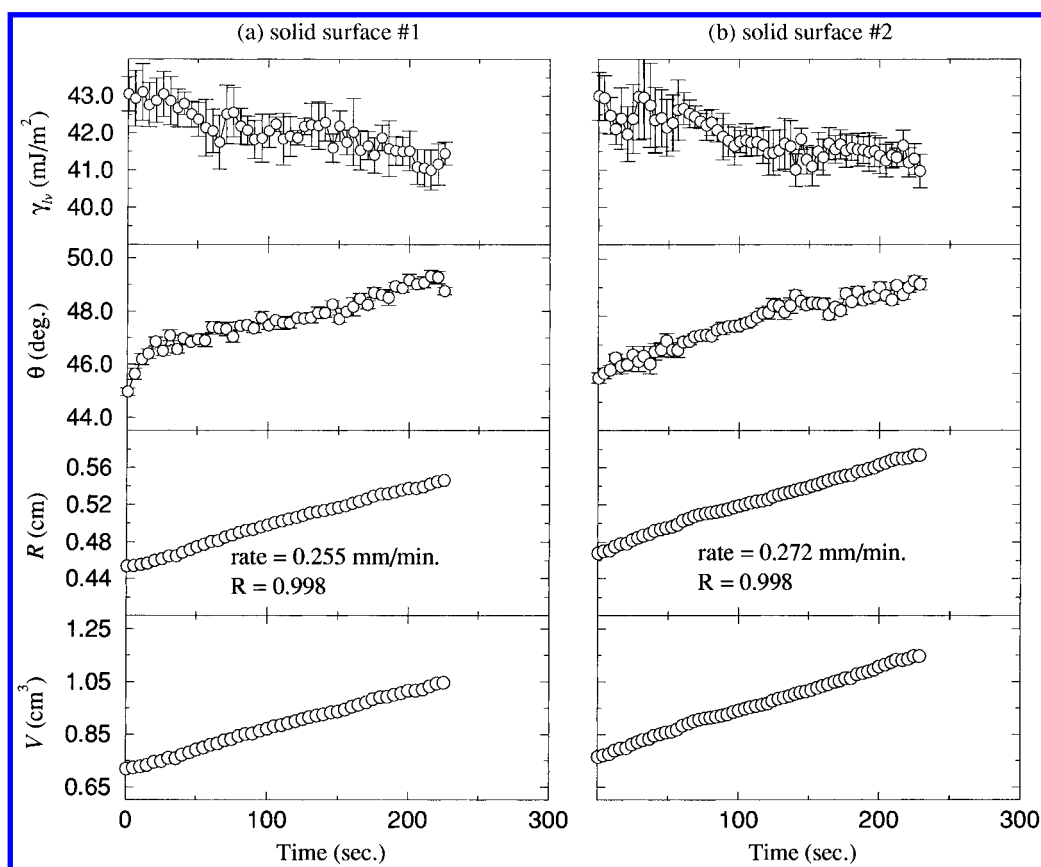


**Figure 8.** Low-rate dynamic contact angles of diethylene glycol on poly(propene-*alt*-*N*-(*n*-propyl)maleimide) copolymer measured by ADSA-P. It is suspected that the solid-liquid (and/or solid-vapor) interfacial tensions are changed slowly due to physicochemical reaction (see text).



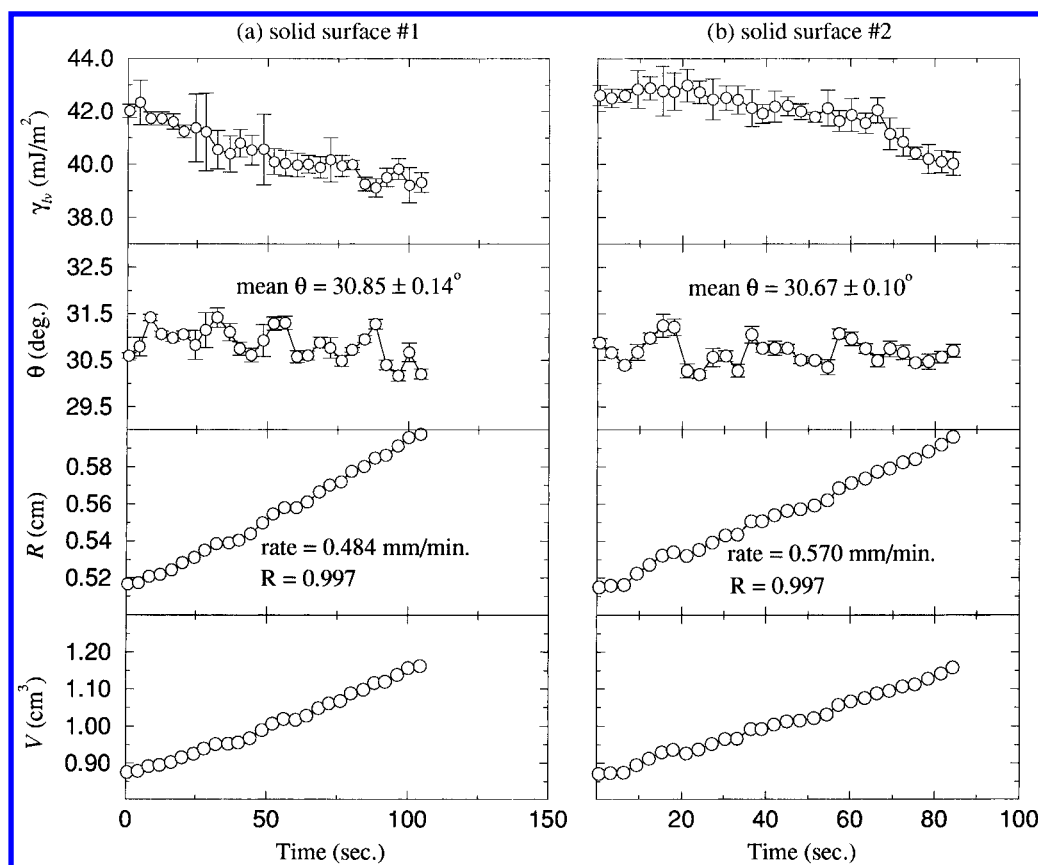


**Figure 9.** Low-rate dynamic contact angles of 1-bromonaphthalene on poly(propene-*alt*-*N*-(*n*-propyl)maleimide) copolymer measured by ADSA-P.

contact angles in Figure 8 should not be used for the interpretation in terms of surface energetics, based on the experimental reason given above and the statistical reasons given in the Appendix.

Figure 9 shows the contact angle results of 1-bromonaphthalene for two different experiments. It can be seen in Figure 9a that the contact angles are essentially constant as the three-phase contact line advances. However, the apparent liquid-vapor surface tension decreases slightly as the three-phase contact line moves. This effect could be due to a tendency toward lack of symmetry of the drop profile for low contact angles, say less than about 30°. This is further supported by the slight nonlinearity in the apparent drop volume and apparent drop contact radius, with a slightly lower regression coefficient. Averaging the contact angles yields a mean  $\theta$  of  $30.85 \pm 0.14^\circ$  at a rate of 0.48 mm/min. Similar results for another experiment, at a different rate of advancing, are shown in Figure 9b. A total of nine experiments at different rates of advancing were performed, and the results are summarized in Table 2.

A summary of the contact angle behavior for all liquids on poly(propene-*alt*-*N*-(*n*-propyl)maleimide) is shown in Table 3. While the contact angle data of formamide, diiodomethane, ethylene glycol, and diethylene glycol should be disregarded for the reasons explained earlier, the contact angles of water, glycerol, thiodiethanol, and 1-bromonaphthalene can be used for the interpretation in terms of surface energetics.

*Poly(propene-*alt*-*N*-(*n*-hexyl)maleimide).* A similar study was conducted for a second copolymer, poly(propene-*alt*-*N*-(*n*-hexyl)maleimide). Only the advancing contact angles of water, glycerol, diethylene glycol, and *cis*-decalin were found to be essentially constant. The remaining liquids, formamide, thiodiethanol, diiodomethane, ethylene glycol, 1-bromonaphthalene, DMSO, dibenzylamine, ethyl cinamate, and dichlorotoluene, all show very complex

**Table 3. Summary of the Contact Angles Measured by ADSA-P on Poly(propene-*alt*-*N*-(*n*-propyl)maleimide Copolymer Surface**

liquids	surface tension $\gamma_{lv}$ (mJ/m <sup>2</sup> )	contact angle $\theta$ (deg)
1-bromonaphthalene	44.31	30.75
diethylene glycol	44.68	$\theta \uparrow$ as $R \uparrow$ ( $45^\circ \rightarrow 49^\circ$ )
ethylene glycol	47.55	$\theta \uparrow$ as $R \uparrow$ ( $54^\circ \rightarrow 57^\circ$ )
diiodomethane	49.98	slip/stick ( $45^\circ \rightarrow 80^\circ$ )
thiodiethanol	56.26	54.04
formamide	59.08	$\theta \downarrow$ and $\gamma \downarrow$ as $R \uparrow$ ( $62^\circ \rightarrow 54^\circ$ )
glycerol	65.02	70.67
water	72.70	77.51

contact angle patterns which force us to exclude these results from the interpretation in terms of surface energetics and the testing of approaches for interfacial tensions.

The contact angle results of water are shown in Figure 10. In Figure 10a, after the initial increase in the water contact angles due to evaporation after deposition of the initial liquid drop, the contact angles are found to be essentially constant as a function of surface location. Averaging these contact angles yields a mean  $\theta$  of  $92.37 \pm 0.08^\circ$  at a rate of 0.08 mm/min. Another experimental result for a new surface is shown in Figure 10b. The apparent contact angles in this case are also very constant, yielding a mean  $\theta$  of  $92.31 \pm 0.10^\circ$  at a rate of 0.07 mm/min. Five low-rate dynamic contact angle experiments were performed in total for this solid-liquid system. They are summarized in Table 4.

Figure 11 shows glycerol contact angle results on poly(propene-*alt*-*N*-(*n*-hexyl)maleimide). It can be seen that the contact angles are essentially constant for two different experiments (rates of advancing), regardless of surface location. The mean contact angles are found to be  $83.24 \pm 0.07^\circ$  and  $82.94 \pm 0.05^\circ$ , respectively, at rates of

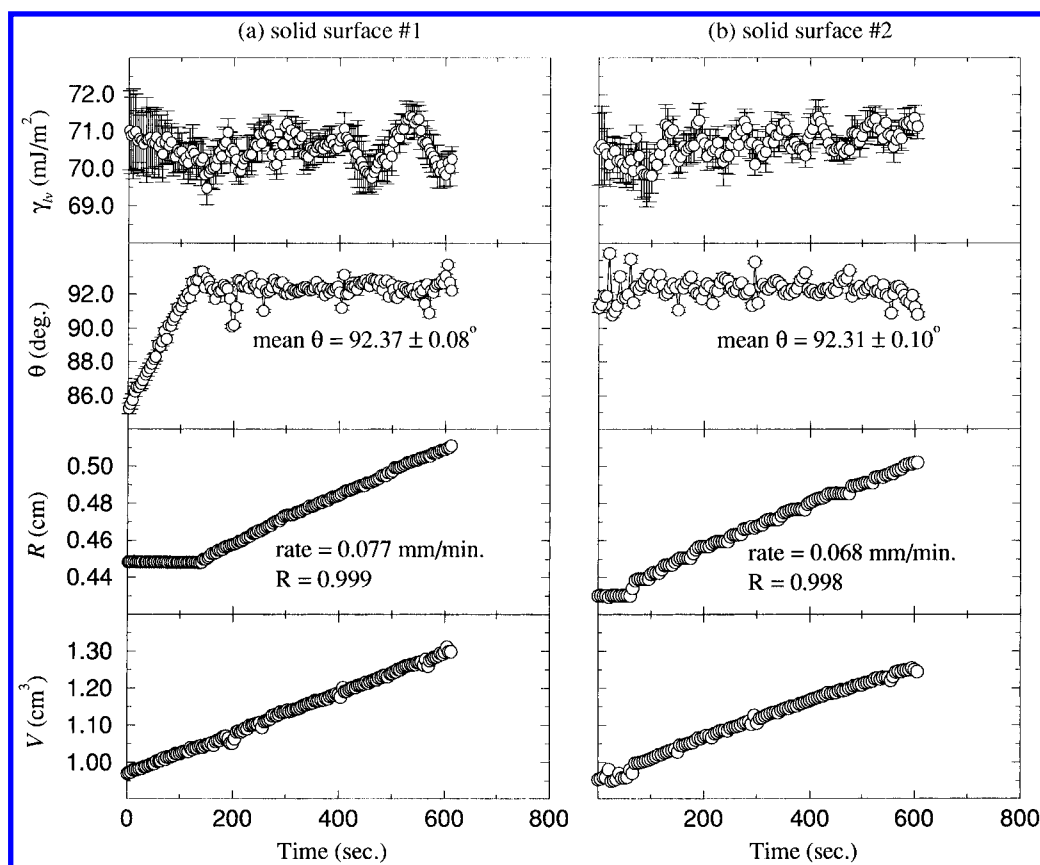


**Figure 10.** Low-rate dynamic contact angles of water on poly(propene-*alt*-*N*-(*n*-hexyl)maleimide) copolymer measured by ADSA-P.

**Table 4.** Low-Rate Dynamic Contact Angles of Different Liquids on Poly(propene-*alt*-*N*-(*n*-hexyl)maleimide) Copolymer Surface

water		glycerol		diethylene glycol		<i>cis</i> -decalin	
rate (mm/min)	$\theta$ (deg)	rate (mm/min)	$\theta$ (deg)	rate (mm/min)	$\theta$ (deg)	rate (mm/min)	$\theta$ (deg)
0.060	92.44	0.082	82.69	0.119	60.75	0.298	28.69
0.068	92.31	0.106	82.97	0.124	60.43	0.335	28.19
0.077	92.37	0.123	82.78	0.186	61.58	0.338	28.96
0.127	91.91	0.145	83.22	0.222	61.18	0.408	28.59
0.150	92.27	0.147	83.24	0.230	61.06	0.459	29.66
		0.162	82.92	0.257	61.45		
		0.164	82.90	0.305	61.21		
		0.226	82.43	0.325	60.84		
		0.244	82.17	0.332	60.89		
		0.275	82.94	0.345	60.96		
92.26 ± 0.26 <sup>a</sup>		82.83 ± 0.24 <sup>a</sup>		61.04 ± 0.24 <sup>a</sup>		28.81 ± 0.67 <sup>a</sup>	

<sup>a</sup> Mean values.

advancing of 0.15 and 0.28 mm/min. Other results are reported in Table 4 for different rates of advancing.

The contact angle results of diethylene glycol are shown in Figure 12. It can be seen that the contact angles for the two experiments are essentially constant. Although it seems that the contact angle tends to increase slightly with  $R$ , the effect is not pronounced and therefore disregarded. The average contact angles are  $61.21 \pm 0.13^\circ$  and  $60.89 \pm 0.10^\circ$ , respectively, at rates of advancing of 0.31 and 0.33 mm/min. Table 4 summarizes the results for different rates of advancing.

Another liquid which results in essentially constant advancing contact angles is *cis*-decalin. Results are shown in Figure 13 for two different experiments. It can be seen that the liquid-vapor surface tensions and contact angles are essentially constant, giving  $\theta$  of  $28.59 \pm 0.06^\circ$  and  $28.69 \pm 0.05^\circ$ , respectively, at rates of advancing of 0.41 and 0.30 mm/min. A total of five experiments for *cis*-decalin were performed, and the results are summarized in Table 4.

The remaining liquids show very complex contact angle

behavior which does not allow us to use these angles for the interpretation in terms of surface energetics. First, it was found that formamide dissolved the poly(propene-*alt*-*N*-(*n*-hexyl)maleimide) copolymer surface on contact, resulting in a very irregular and flat drop. In the case of thiodiethanol in Figure 14a, slip/stick occurs. Initially the contact angle increases from about  $65^\circ$  to  $90^\circ$  at essentially constant three-phase contact radius. As more liquid is supplied into the sessile drop, the drop front slips, causing a sudden decrease in the contact angle from  $90^\circ$  to  $65^\circ$ . Figure 14b shows a similar slip/stick behavior for diiodomethane. For ethylene glycol, shown in Figure 14c, the contact angle increases slowly from about  $67^\circ$  to  $70^\circ$ . Again this is similar to the contact angle patterns shown in Figures 7 and 8 on the poly(propene-*alt*-*N*-(*n*-propyl)maleimide) copolymer surface. In addition to the experimental reasons given above, a statistical reason to reject these angles is also discussed in the Appendix. Figure 14d shows a contact angle result of 1-bromonaphthalene where the liquid-vapor surface tension decreases from 43 to about 37 mJ/m<sup>2</sup> and the contact angle increases

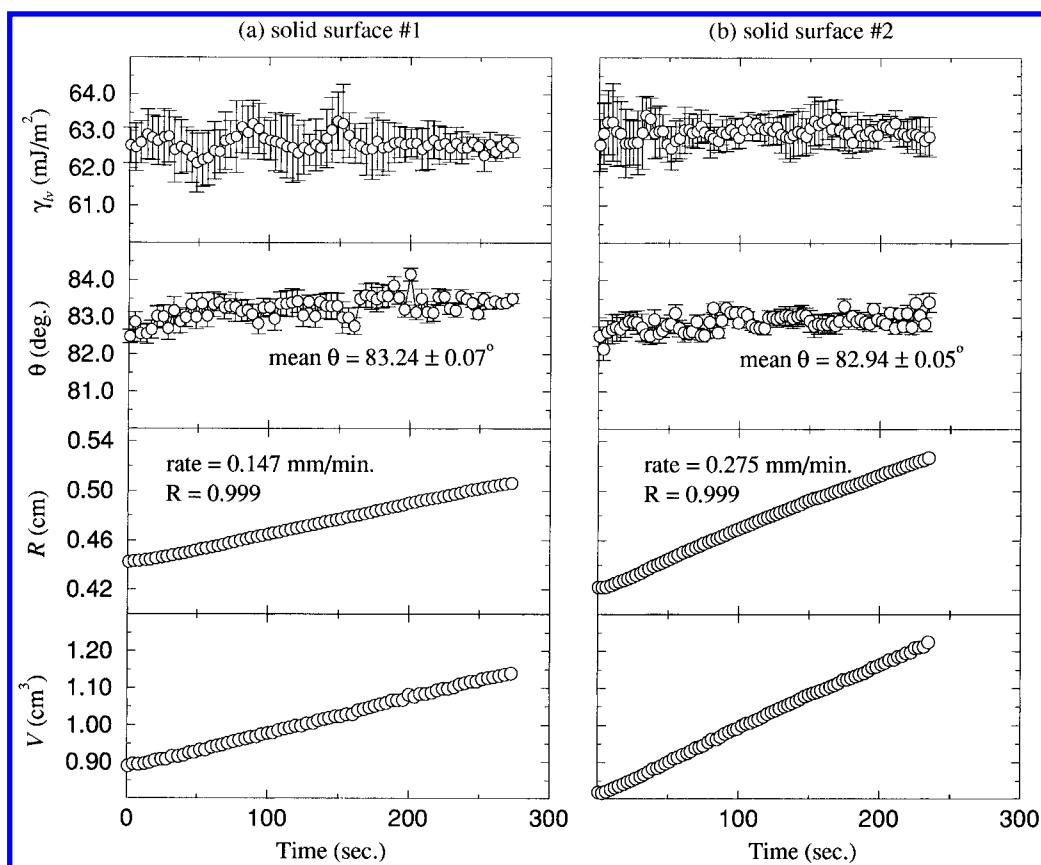


**Figure 11.** Low-rate dynamic contact angles of glycerol on poly(propene-*alt*-*N*-(*n*-hexyl)maleimide) copolymer measured by ADSA-P.

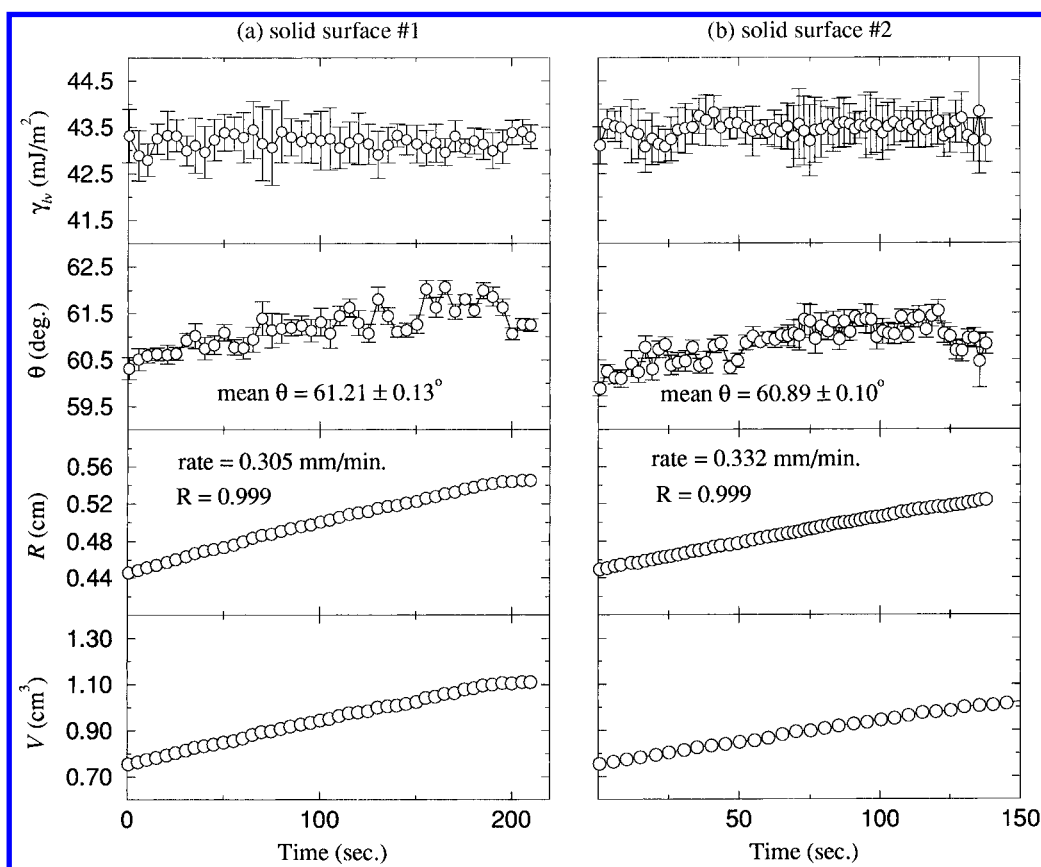


**Figure 12.** Low-rate dynamic contact angles of diethylene glycol on poly(propene-*alt*-*N*-(*n*-hexyl)maleimide) copolymer measured by ADSA-P.

from about 40° to 60° as  $R$  increases. Such a pattern is likely to be caused by the dissolution of the copolymer by the liquid. A similar example is shown in Figure 14e for

DMSO. It can be seen that the observed surface tension of DMSO is lower than what it should be for a pure liquid by about 9 mJ/m<sup>2</sup>. This may suggest dissolution of the

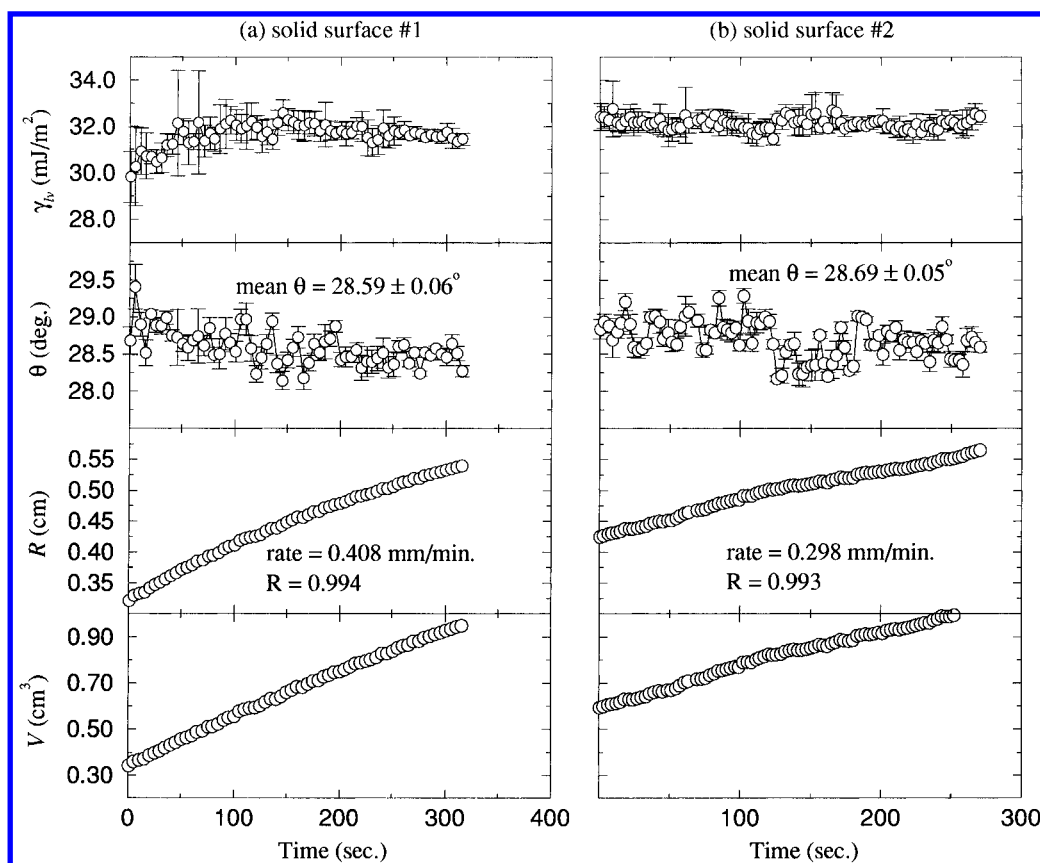


**Figure 13.** Low-rate dynamic contact angles of *cis*-decalin on poly(propene-*alt*-*N*-(*n*-hexyl)maleimide) copolymer measured by ADSA-P.

copolymer by DMSO immediately after drop formation. Such a physicochemical reaction reduces the surface tension of DMSO. However, as the drop volume continues to increase linearly up to 600 s, the three-phase contact line moves by only 0.1 cm. This causes  $\theta$  to increase from 40° to 65°. Such a behavior could be due to both dissolution as well as slip/stick, which causes  $\theta$  to increase at essentially constant  $R$ . Additional increase in the drop volume and hence the three-phase contact area (radius) causes the surface tension of DMSO to decrease further by 1 mJ/m<sup>2</sup>, since more copolymer is available for DMSO to dissolve. Beyond 600 s, the changes in the apparent drop volume and three-phase contact radius do not behave linearly and, therefore, the symmetry of the sessile drop is no longer preserved. Indeed, it was observed after the experiment that the copolymer layer in the area of contact between DMSO and the copolymer appeared to be partly removed. Figure 14f shows the contact angle result of dibenzylamine, where the liquid–vapor surface tension decreases by 2 mJ/m<sup>2</sup> and the contact angle decreases from 39° to 34°. It is suspected again that a physicochemical reaction takes place in this system. This changes the solid–liquid interfacial tension and possibly the solid–vapor interfacial tension, as discussed before. A statistical reason to reject these angles is also discussed in the Appendix. Figure 14g shows the contact angle results of ethyl cinnamate, where the surface tension/contact angle behavior is similar to that of Figure 14f: in Figure 14g, the surface tension decreases from about 35 to 29 mJ/m<sup>2</sup> and the contact angle decreases from 66° to 56°. In the case of dichlorotoluene in Figure 14h, the contact angle increases from 29° to 37° with a slight decrease in the liquid–vapor surface tension.

A summary of the contact angle behavior for all 13 liquids on poly(propene-*alt*-*N*-(*n*-hexyl)maleimide) is shown in Table 5. It is obvious that only the contact angles of water, glycerol, diethylene glycol, and *cis*-decalin can be

**Table 5. Summary of the Contact Angles Measured by ADSA-P on Poly(propene-*alt*-*N*-(*n*-hexyl)maleimide) Copolymer Surface**

liquids	surface tension $\gamma_{lv}$ (mJ/m <sup>2</sup> )	contact angle $\theta$ (deg)
<i>cis</i> -decalin	32.32	28.81
2,5-dichlorotoluene	34.64	$\theta \uparrow$ as $R \uparrow$ (29° → 37°)
ethyl cinnamate	37.17	$\theta \downarrow$ and $\gamma \downarrow$ as $R \uparrow$ (66° → 56°)
dibenzylamine	40.80	$\theta \downarrow$ and $R \uparrow$ (39° → 34°)
DMSO	42.68	$\theta \uparrow$ and $\gamma \downarrow$ as $R \uparrow$ (40° → 65°)
1-bromonaphthalene	44.31	$\theta \uparrow$ and $\gamma \downarrow$ as $R \uparrow$ (40° → 60°)
diethylene glycol	44.68	61.04
ethylene glycol	47.55	$\theta \uparrow$ as $R \uparrow$ (67° → 70°)
diiodomethane	49.98	slip/stick (88° → 96°)
thiodiethanol	56.26	slip/stick (68° → 90°)
formamide	59.08	formamide dissolved the polymer on contact
glycerol	65.02	82.83
water	72.70	92.26

used for the interpretation in terms of surface energetics. The remaining liquids show very complex contact angle behavior.

**Goniometer Measurements.** For comparison purposes, we have also measured advancing contact angles using a conventional goniometer technique. The procedures are as follows: A sessile drop of about 0.4–0.5 cm radius was formed from above. The three-phase contact line of the drop was then slowly advanced by supplying more liquid from above through a capillary which was always kept in contact with the drop. The maximum (advancing) contact angles were measured carefully from the left and right side of the drop and subsequently averaged. The above procedures were repeated for five drops on five new surfaces. All readings were then averaged to give an averaged contact angle. The results, together with those from ADSA-P (in Tables 3 and 5), are summarized in Table 6. As can be seen in this table, the

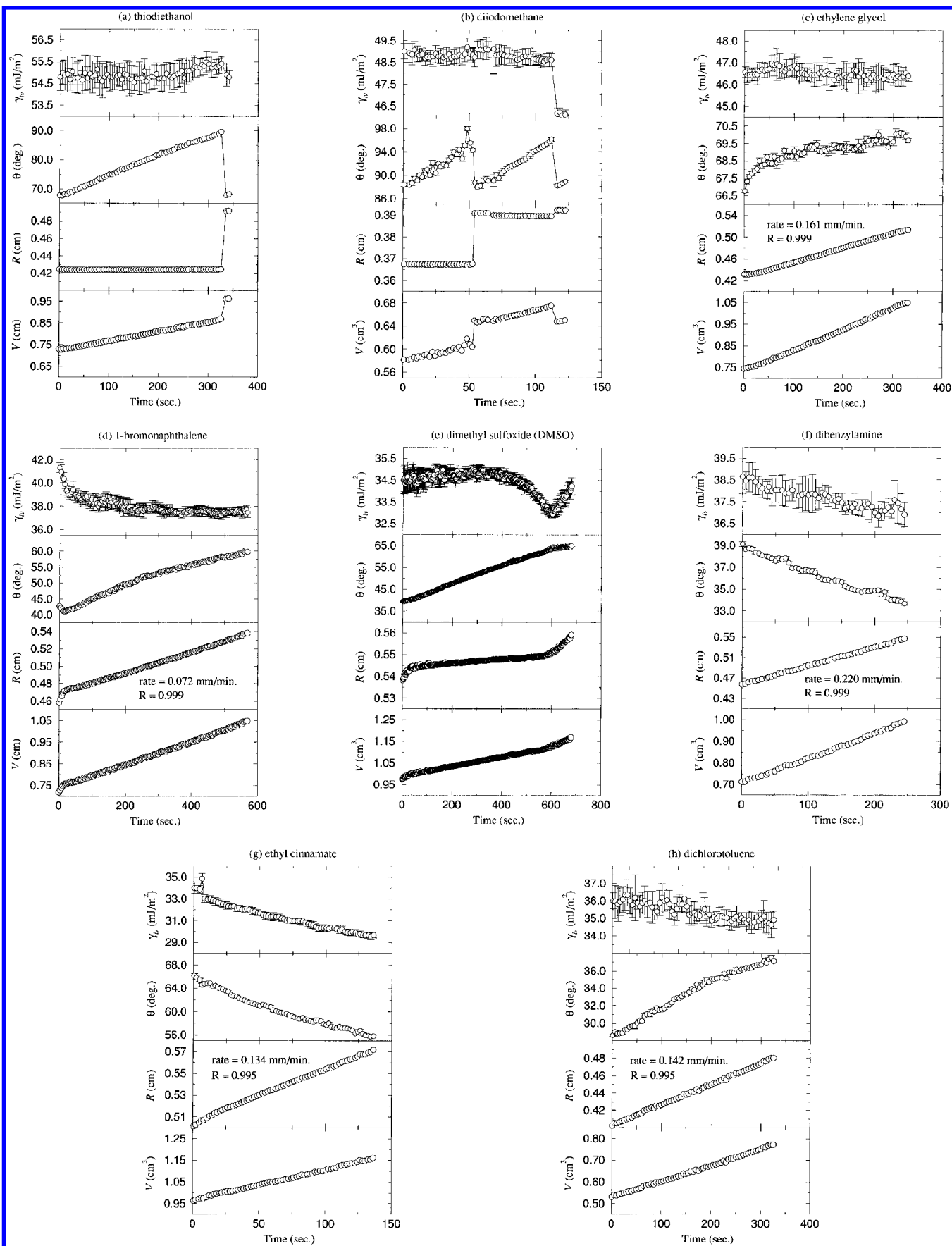


**Figure 14.** Low-rate dynamic contact angles of (a) thiodiethanol, (b) diiodomethane, (c) ethylene glycol, (d) 1-bromonaphthalene, (e) DMSO, (f) dibenzylamine, (g) ethyl cinnamate, and (h) dichlorotoluene on poly(propene-*alt*-N-(*n*-hexyl)maleimide) copolymer measured by ADSA-P. These experimental contact angles should be disregarded for the interpretation of surface energetics, since it is unsure whether or not Young's equation is applicable and whether these solid-liquid systems violate the basic assumptions made in all surface energetics approaches<sup>1-8</sup> (see text).

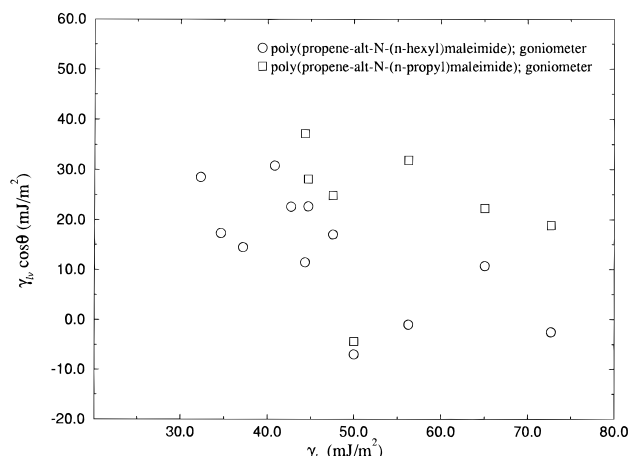
contact angles observed by the goniometer technique and ADSA-P are virtually identical for solid-liquid systems

which have essentially constant contact angles. However, for solid-liquid systems which are complex, only the



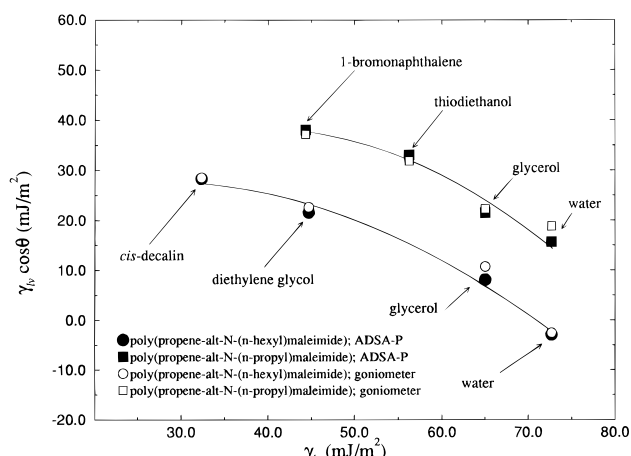
**Table 6.** Comparison between the Advancing Contact Angles (degrees) Measured by ADSA-P and a Goniometer on Two Copolymer Surfaces: Poly(propene-*alt*-N-(*n*-propyl)maleimide) and Poly(propene-*alt*-N-(*n*-hexyl)maleimide)

liquids	poly(propene- <i>alt</i> -N-( <i>n</i> -propyl)maleimide)		poly(propene- <i>alt</i> -N-( <i>n</i> -hexyl)maleimide)	
	ADSA-P	goniometer	ADSA-P	goniometer
<i>cis</i> -decalin			28.81	28.0
2,5-dichlorotoluene			$\theta \uparrow$ as $R \uparrow$ (29° → 37°)	60.0
ethyl cinnamate			$\theta \downarrow$ and $\gamma \downarrow$ as $R \uparrow$ (66° → 56°)	67.0
dibenzylamine			$\theta \downarrow$ and $R \uparrow$ (39° → 34°)	41.0
DMSO			$\theta \uparrow$ and $\gamma \downarrow$ as $R \uparrow$ (40° → 65°)	58.0
1-bromonaphthalene	30.75	33.0	$\theta \uparrow$ and $\gamma \downarrow$ as $R \uparrow$ (40° → 60°)	75.0
diethylene glycol	$\theta \uparrow$ as $R \uparrow$ (45° → 49°)	51.0	$\theta \uparrow$ as $R \uparrow$ (67° → 70°)	59.5
ethylene glycol	$\theta \uparrow$ as $R \uparrow$ (54° → 57°)	58.5	slip/stick (88° → 96°)	69.0
diiodomethane	slip/stick (45° → 80°)	95.0	slip/stick (68° → 90°)	98.0
thiodiethanol	54.04	55.5	formamide dissolved the polymer	91.0
formamide	$\theta \downarrow$ and $\gamma \downarrow$ as $R \uparrow$ (62° → 54°)	67.0	on contact	
glycerol	70.67	70.0	82.83	80.5
water	77.51	75.0	92.26	92.0

**Figure 15.** Values of  $\gamma_{lv} \cos \theta$  vs  $\gamma_{lv}$  obtained from the goniometer study, for the poly(propene-*alt*-N-(*n*-propyl)maleimide) and poly(propene-*alt*-N-(*n*-hexyl)maleimide) copolymers. Data are from Table 6. Due to the scatters, one might want to conclude that the values of  $\gamma_{lv} \cos \theta$  may depend on various parameters such as intermolecular forces, in addition to  $\gamma_{lv}$  and  $\gamma_{sv}$ .

maximum (advancing) contact angle is normally recorded by the goniometer technique. While pronounced cases of slip/stick behavior can indeed be observed by the goniometer, it is virtually impossible to record the entire slip/stick behavior manually. While these maximum contact angles are the advancing contact angles, they cannot be used for the interpretation in terms of surface energetics due to obvious reasons discussed earlier. This distinction and differentiations made in the ADSA-P study are not possible in the goniometer study. Of course, a contact angle thus recorded by the goniometer should agree with maximum angles obtained by ADSA-P. For example, for diiodomethane on the poly(propene-*alt*-N-(*n*-hexyl)maleimide) copolymer surface, the goniometer value is 98°, in agreement with the maxima in the entire slip/stick pattern ADSA-P results ( $\theta \approx 96^\circ$ ) in Figure 14b. It is obvious that a simple contact angle technique, e.g., a goniometer, cannot reflect the complexities of solid-liquid interactions such as slip/stick mechanisms and physicochemical reactions. In the cases where the liquid-vapor surface tension of the sessile drop decreases due to dissolution of the surface, it is impossible for a goniometer type of technique to detect changes in the liquid-vapor surface tension. Conventional goniometer contact angle measurements are liable to produce a mixture of meaningful and meaningless contact angle data, with no criteria to distinguish between the two.

**Comparison between ADSA-P and Goniometer Results.** If the contact angle data (in Table 6) from the goniometer study are plotted as  $\gamma_{lv} \cos \theta$  vs  $\gamma_{lv}$ , no obvious

**Figure 16.** Values of  $\gamma_{lv} \cos \theta$  vs  $\gamma_{lv}$  from the ADSA-P and goniometer study for the poly(propene-*alt*-N-(*n*-propyl)maleimide) and poly(propene-*alt*-N-(*n*-hexyl)maleimide) copolymers. The goniometer contact angle data are reproduced from Figure 15 by excluding the inconclusive contact angles shown to be meaningless in the ADSA-P study. This result suggests that, for a given solid surface (i.e., constant  $\gamma_{sv}$ ), the values of  $\gamma_{lv} \cos \theta$  depend only on the liquid-vapor surface tensions,  $\gamma_{lv}$ , regardless of intermolecular forces which give rise to the surface tensions.

functional dependence can be observed. One might want to conclude from Figure 15 that the values of  $\gamma_{lv} \cos \theta$  may depend on various parameters, in addition to  $\gamma_{lv}$  and  $\gamma_{sv}$ , such as specific intermolecular forces. These patterns arise from the fact that, other than the validity of Young's equation, the assumptions of the constancy of  $\gamma_{lv}$  for a given liquid and the constancy of  $\gamma_{sv}$  going from liquid to liquid (or  $\gamma_{sl} = \text{constant}$ , i.e., invariant with time) are violated, and they cannot be easily detected using a conventional goniometer-sessile drop technique. The picture, however, changes drastically (see Figure 16) upon elimination of the angles (in Figure 15) shown to be meaningless in the ADSA-P study. The curves in Figure 16 are in perfect harmony with the results obtained for more inert polar and nonpolar surfaces.<sup>14,26,27</sup>

## Conclusions

- (1) Contact angle phenomena are complicated.
- (2) Circumspection is necessary in the decision whether or not experimental contact angles can be used in conjunction with Young's equation.
- (3) Low-rate dynamic contact angle measurement from ADSA-P allows one to distinguish good contact angles from bad ones on noninert surfaces.

(26) Li, D.; Neumann, A. W. *J. Colloid Interface Sci.* **1992**, *148*, 190.

(27) Kwok, D. Y.; Li, D.; Neumann, A. W. *Colloids Surf. A* **1994**, *89*, 181.



**Table 7. Summary of the Correlation Analysis To Study whether or Not Averaging the Contact Angles over Time Is Allowed for the Solid–Liquid Systems in Figures 2a, 7a–b, 8a–b, 10a, 14c, and 14f**

	no. of observations after $R = 0.48$ cm	$r_{\text{cal}}$	$r_{\text{tab}}$ at 99%	is averaging allowed at 99% confidence?
Poly(propene- <i>alt</i> - <i>N</i> -( <i>n</i> -propyl)maleimide)				
ethylene glycol in Figure 7a	73	0.935	0.29	no
ethylene glycol in Figure 7b	86	0.960	0.27	no
diethylene glycol in Figure 8a	34	0.949	0.43	no
diethylene glycol in Figure 8b	52	0.960	0.35	no
water in Figure 2a	62	−0.048	0.33	yes
Poly(propene- <i>alt</i> - <i>N</i> -( <i>n</i> -hexyl)maleimide)				
ethylene glycol in Figure 14c	34	0.830	0.43	no
dibenzylamine in Figure 14f	38	−0.981	0.40	no
water in Figure 10a	63	0.084	0.33	yes

(4) Caution should be exercised when measuring and interpreting static advancing contact angles using a goniometer technique on noninert surfaces.

(5) Contact angles from a conventional goniometer–sessile drop technique may produce contact angles which violate the basic assumptions made in all surface energetics approaches,<sup>1–8</sup> e.g., constancy of  $\gamma_{\text{sv}}$ .

(6) If one omits the inconclusive contact angle measurements, the values of  $\gamma_{\text{lv}} \cos \theta$  change smoothly with  $\gamma_{\text{lv}}$  for copolymers with polar groups, here poly(propene-*alt*-*N*-(*n*-propyl)maleimide and poly(propene-*alt*-*N*-(*n*-hexyl)maleimide, in the same fashion as for nonpolar polymers.

**Acknowledgment.** This research was supported by the Natural Science and Engineering Research Council of Canada (Grants A8278 and no EQP173469), a Ontario Graduate Scholarship (D.Y.K.), and a University of Toronto Open Fellowship (D.Y.K.).

### Appendix

In the analysis of experimental data, it is desirable to study whether correlation exists among variables and, if so, how one variable correlates (or associates) with the others. For example, one might ask what is the association between surface tension and temperature? Does one depend on the other, or are they unrelated? These situations are covered by correlation analysis.<sup>28</sup> In other situations, one may be interested in establishing the functional relationship among the variables, where regression analysis applies.<sup>28</sup> In the above example, one might ask, alternatively, what is the functional relationship between surface tension and temperature. However, a functional relationship must be assumed, *a priori*. Once the functional relationship is established between the independent and dependent variables, regression analysis can be used to determine how well this relation fits the experimental data. For example, regression analysis can be used to determine whether a straight line or a quadratic equation should be used to best describe the dependence of surface tension on the temperature.

(28) Lipson, C.; Sheth, N. J. *Statistical Design and Analysis of Engineering Experiments*; McGraw-Hill Publishing Co.: New York, 1973; Chapter 13, p 372.

For the purpose of studying whether averaging of contact angles over time is allowed, correlation analysis is used since one does not have to assume a functional relationship between contact angle and time: All we want to know is whether the experimental contact angle is associated with time for a specific experiment, and if so, averaging is not allowed. A quantitative measure of the association between the variables is defined by the correlation coefficient,  $r$ . The range of  $r$  can be from  $-1$  to  $+1$ , depending on the degree of association. For example, when  $r = -1$ , a perfect, but negative, correlation exists among the variables. Statistical tables<sup>28</sup> can be used to determine the significance of the calculated correlation coefficient,  $r_{\text{cal}}$ , from a sample at a certain confidence level. Such table provides the maximum values of  $r_{\text{tab}}$  which can be expected by chance alone when actually no correlation exists. In order to conclude at a given confidence level that correlation does exist, the calculated  $r_{\text{cal}}$  should exceed the tabulated value of  $r_{\text{tab}}$ .

In Figure 7a, the calculated correlation coefficient,  $r_{\text{cal}}$ , is found to be 0.935, where the tabulated correlation coefficient,  $r_{\text{tab}}$ , at 99% confidence is found to be 0.29 (see Table 7). Since  $r_{\text{cal}} = 0.935 \gg r_{\text{tab}} = 0.29$ , one can conclude that, at 99% confidence, contact angle and time are strongly correlated. The positive value of  $r_{\text{cal}}$  indicates that contact angle and time are correlated positively. Thus, averaging of contact angles over time in Figure 7a is not allowed. Similar conclusions with similar results (see Table 7) can be drawn for other liquids in Figures 7b, 8a–b, 14c, and 14f, where controversy might arise as to whether averaging is allowed, if only the experimental reasons discussed earlier in the paper are considered.

To prove our point, the correlation coefficients for water on poly(propene-*alt*-*N*-(*n*-propyl)maleimide) in Figure 2a and water on poly(propene-*alt*-*N*-(*n*-hexyl)maleimide) in Figure 10a, respectively, were also calculated. In both cases, the calculated correlation coefficients,  $r_{\text{cal}}$ , are significantly less than those of the  $r_{\text{tab}}$  at 99% confidence (see Table 7). Thus, one can conclude that at 99% confidence, there is no correlation between the contact angle and time and averaging the contact angles over time is allowed.

LA9608021